

MASSIVE FIELD STARS AND THE STELLAR CLUSTERING LAW

M. S. OEY AND N. L. KING

Lowell Observatory, 1400 W. Mars Hill Rd., Flagstaff, AZ 86001; Sally.Oey@lowell.edu

AND

J. WM. PARKER

Department of Space Studies, Southwest Research Institute, Suite 426, 1050 Walnut St., Boulder, CO 80302

Accepted to the ASTRONOMICAL JOURNAL 26 November 2003

ABSTRACT

The distribution of N_* , the number of OB stars per association or cluster, appears to follow a universal power-law form N_*^{-2} in the local Universe. We evaluate the distribution of N_* in the Small Magellanic Cloud using recent broadband optical and space-ultraviolet data, with special attention to the lowest values of N_* . We find that the power-law distribution in N_* continues smoothly down to $N_*=1$. This strongly suggests that the formation of field massive stars is a continuous process with those in associations, and that the field stars do not originate from a different star formation mode. Our results are consistent with the model that field massive stars represent the most massive members in groups of smaller stars, as expected if the clustering law applies to much lower masses as is expected from the stellar initial mass function (IMF). These results are consistent with the *simultaneous* existence of a universal IMF and a universal clustering law. Jointly, these laws imply that the fraction of field OB stars typically ranges from about 35% to 7% for most astrophysical situations, with an inverse logarithmic dependence on the most populous cluster, and hence, on galaxy size and/or star formation rate. There are important consequences for global feedback effects in galaxies: field stars should therefore contribute proportionately to the volume of the warm ionized medium, and equal relative contributions by superbubbles of all sizes to the interstellar porosity are expected.

Subject headings: stars: early-type — stars: formation — stars: statistics — galaxies: star clusters — galaxies: stellar content — galaxies: individual (SMC)

1. INTRODUCTION

It is commonly held that most massive, OB stars are found in stellar clusters, or associations, since their short (~ 10 Myr) lifetimes are not long enough to permit spatial dispersion from their natal companions. However, apparently-isolated, massive field stars are well-known to exist, including a class of runaway OB stars with unusually large ($\gtrsim 30$ km s⁻¹) velocities. While runaway OB stars are generally believed to be kinematically ejected from a parent OB association, the ordinary non-runaway field OB stars have been suggested to originate in a different mode of star formation from their counterparts in associations. Suggested differences between clusters and the field in the stellar initial mass function (IMF) for high-mass stars (Massey 2002; Kroupa & Weidner 2003) support this possibility. This contribution explores the relationship between OB associations and massive field stars.

In recent years, it has emerged that the number of stars N_* per cluster appears to follow a universal power law distribution:

$$N(N_*) dN_* \propto N_*^{-2} dN_* \quad . \quad (1)$$

This has been found empirically for young, massive clusters (e.g., Hunter et al. 2003; Zhang & Fall 1999), super star clusters (Meurer et al. 1995), globular clusters (e.g., Harris & Pudritz 1994) and H II regions (Oey & Clarke 1998). The apparent universality of this relation is emerging as fundamental (e.g., Oey & Muñoz-Tuñon 2003; Oey & Clarke 1998; Elmegreen & Efremov 1997), similar to the constant power-law relation for the IMF. If individual,

field OB stars have a fundamentally different origin from clustered OB stars, then this is likely to be manifest in the distribution of N_* , near $N_* = 1$, where N_* specifically counts massive stars only (here, $m \gtrsim 10 M_\odot$). In what follows, we examine the form of $N(N_*)$, for small N_* , a regime that has not been investigated to date, to illuminate the relationship between massive star clustering and massive field stars.

2. THE SMC SAMPLE OF OB STARS

A study of OB star clustering properties and field stars requires high spatial resolution and essentially complete detection of the OB stars over a large area of a given galaxy. The Magellanic Clouds are optimal target galaxies by virtue of their proximity and high Galactic latitude. Indeed, some of the earliest work on OB associations and massive star censuses was carried out for the Magellanic Clouds by Feast et al. (1960), Sanduleak (1969), Lucke & Hodge (1970), Azzopardi & Vigneanu (1982), and Hodge (1985). More recently, the *UBVR* survey data of Massey (2002) for the Small Magellanic Cloud (SMC), together with UV photometry (Parker et al. 1998) from the *Ultraviolet Imaging Telescope (UIT)*, provide unprecedented depth, resolution, completeness, and broadband coverage for the massive star population over a large fraction of the SMC. The area observed by *UIT* is smaller than the optical survey, but covers the SMC bar, which includes most of the active star formation in that galaxy. Figure 1 shows the regions covered by the two surveys. SMC OB associations have previously been identified and catalogued by Hodge

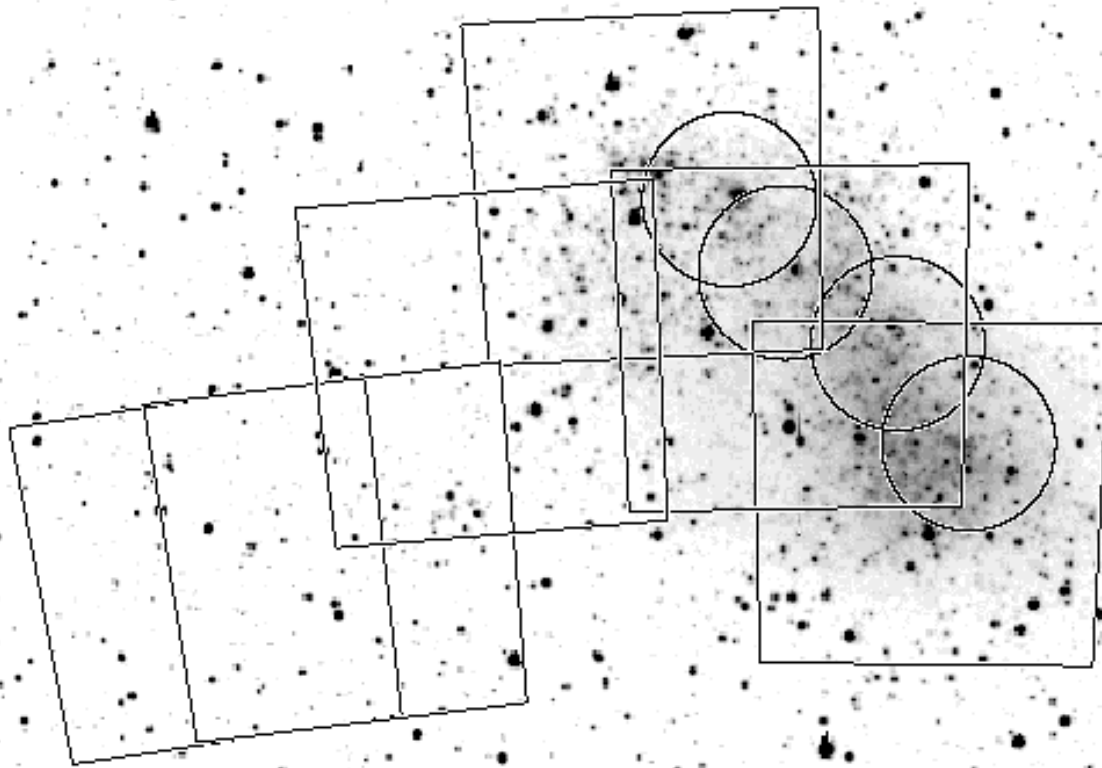


FIG. 1.— Grayscale R -band image of the SMC (Bothun & Thompson 1988) showing the area coverage for the $UBVR$ survey (Massey et al. 2002; rectangular regions) and the UIT survey (Parker et al. 1998; circular regions). The optical fields are $79'$ square, and the UIT fields are $37'$ in diameter. North is up, east to the left.

(1985) and Battinelli (1991), the latter from the photographic OB census of Azzopardi & Vigneanu (1982). Here, we re-examine the clustering properties of these massive stars in the SMC, using the modern datasets to first systematically identify OB stars, and then to systematically identify groups or associations of them. We will especially focus on the statistical properties of the low- N_* regime.

Parker et al. (1998) provide UIT photometry in the B5 filter ($\lambda_{\text{eff}} = 1615 \text{ \AA}$, $\Delta\lambda = 225 \text{ \AA}$), which recently has been recalibrated by Parker, Cornett, & Stecher (2004, in preparation). The $UBVR$ photometry of Massey (2002) was observed through a Harris filter set and transformed to the Johnson-Cousins system (Landolt 1992). Reddening-free Q indices were computed using the extinction law of Cardelli, Clayton, & Mathis (1989) with a total to selective extinction ratio $R_V = 3.1$. Different combinations of filters were used to best select two different stellar samples: Stars with initial masses $\gtrsim 10 M_\odot$, corresponding to spectral types of B0 V, B0.5 I and earlier, were selected on the basis of their optical photometry only; and stars with initial masses $\gtrsim 20 M_\odot$, corresponding to spectral types of O9 V, B0 I and earlier were selected on the basis of both their $UBVR$ and UIT photometry. We refer to the former as the OB sample, and the latter as the O-star sample, although we emphasize that neither sample consists of spectroscopically confirmed stars. Our criteria are as follows, using an SMC distance modulus $DM = 18.88$ (Dolphin et al. 2001) and global average extinction $A_B = 0.53$:

$$m_B \leq -4.2 + DM + A_B$$

$$\leq 15.21 \quad (2)$$

$$Q_{U-R, B-R} \leq -0.84, \quad (3)$$

$$Q_{B5-U, B-R} \leq -1.45, \quad (4)$$

$$Q_{B5-V, U-V} \leq 0.03, \quad (5)$$

where

$$\begin{aligned} Q_{U-R, B-R} &= (m_U - m_R) - \frac{A_U - A_R}{A_B - A_R} (m_B - m_R) \\ &= (m_U - m_R) - 1.396 (m_B - m_R), \quad (6) \end{aligned}$$

$$\begin{aligned} Q_{B5-U, B-R} &= (m_{B5} - m_U) - \frac{A_{B5} - A_U}{A_B - A_R} (m_B - m_R) \\ &= (m_{B5} - m_U) - 1.668 (m_B - m_R), \quad (7) \end{aligned}$$

$$\begin{aligned} Q_{B5-V, U-V} &= (m_{B5} - m_V) - \frac{A_{B5} - A_V}{A_U - A_V} (m_U - m_V) \\ &= (m_{B5} - m_V) - 2.718 (m_U - m_V). \quad (8) \end{aligned}$$

The OB sample is selected from equations 2 and 3 only, while the O-star sub-sample meets all of equations 2 to 5.

Table 1 shows all the stars having both UIT B5 photometry, $UBVR$ photometry, and spectral classifications listed by Massey (2002), excluding stars with objective prism classifications and those identified as uncertain spectral types. The ID number and classification from Massey (2002) are shown in Columns 1 and 2. Column 3 shows whether the star met the O-star selection criteria above. Our attempts to select only stars earlier than O9 V and B0 I were successful for 27 out of 31 stars; of the 4 not

selected, one had nebular emission affecting the photometry and two others had weak metal lines (designation W in spectral type). The false positives were 8 out of 26 stars; the majority of the false positives were weak lined stars (W), emission line stars, and peculiar stars.

3. IDENTIFICATION OF OB ASSOCIATIONS

Having identified two samples of 1360 OB and 382 O stars, we then used the friends-of-friends algorithm described by Battinelli (1991) to identify the associations of these stars. Our parameter N_* refers specifically to counts of OB stars from these samples, identified as described above. Battinelli’s algorithm adopts as the clustering distance d_s between associated members the value of d_s that maximizes the number of clusters for $N_* \geq 3$. All stars within d_s of another member star are defined to be within the same group. (We do not distinguish between “group,” “association,” and “cluster” in this work.) Figure 2 shows the number of clusters N as a function d_s near the peak in N for the OB sample (Figure 2a) and O-star sample (Figure 2b). For the OB sample, the characteristic $d_s = 28$ pc ($97''$) is straightforward to determine, but for the O-star sample, it is apparent that N is less sensitive to d_s . We adopt $d_s = 34$ pc ($117''$) for the O-star sample, corresponding to the mean value over the considered range; the larger value of d_s as compared to the OB sample is consistent with the lower stellar density for O stars. Although the clustering properties are relatively insensitive to the choice of d_s within a few pc, we caution that larger values of d_s will result in flatter slopes for the clustering law $N(N_*)$ (e.g., equation 1), as discussed below in §4. Our values of d_s are much smaller than Battinelli’s value of 60 pc; this is consistent with a much greater completeness in our data, yielding a higher density of OB stars, and therefore smaller clustering distance.

Table 2 presents the groups having at least 3 stars that are identified from our OB sample. Column 1 shows the group ID number, columns 2 and 3 give the group centroid position in decimal degrees (J2000.0), columns 4 and 5 give the group diameter D in arcmin and pc, respectively, and column 6 lists the number of stars in the group. Table 3 presents the groups identified from the O star sample in the same way. The group diameters are defined as $D = \frac{1}{2}(\Delta\alpha + \Delta\delta)$ following Battinelli (1991), where $\Delta\alpha$ and $\Delta\delta$ represent the maximum difference between members in RA and Dec, respectively, in degrees of arc. We also list the individual member stars for each group in Tables 4 and 5, which are fully available in the on-line edition. The first two columns of Tables 4 and 5 give the RA and Dec of each star in decimal degrees (J2000.0), columns 3 – 10 give the $UBVR$ magnitudes and uncertainties from Massey (2002), and the last two columns give the star ID from Massey (2002) and our newly-determined OB group ID. Table 5 also lists the UIT B5 magnitudes from Parker et al. (2004) in columns 11 and 12. Note that these group identifications represent the results from two separate runs of the group-finding algorithm; thus, if a star belongs to both samples, it may belong to groups in both Table 4 and Table 5.

Figure 3 shows the location of the group centroids compared to those of associations identified by Hodge (1985; solid black circles) and Battinelli (1991; dashed black circles). Our OB and O-star groups are indicated by the solid

blue and red circles, respectively. The circle sizes correspond to the mean diameters D from Tables 2 and 3. For the Hodge objects, the diameters are taken to be the mean of the dimensions in RA and Dec given by Hodge (1985). There is good general correspondence between the positions of our groups and these earlier catalogs; certainly at least as good as the correspondence between the Hodge (1985) and Battinelli (1991) identifications. It is apparent that the net tendency from our smaller d_s is for our associations to be smaller than those in the earlier catalogs, and to break up some of those associations into smaller groups. Figures 4a, c and 4b, d show the size distributions for, respectively, the OB and O-star samples. It is apparent that, aside from individual stars, the peak in the distribution is around 10–15 pc, compared to 50 pc for both the Battinelli (1991) and Hodge (1985) catalogs. Whereas Hodge (1985) reports that the mean diameter of his sample is similar to the mean for the LMC sample, our smaller characteristic value is consistent with the lower luminosities of the SMC H II regions and star-forming regions compared to those of the LMC (e.g., Kennicutt, Edgar, & Hodge 1989).

4. FIELD VS CLUSTERS

Figure 5 shows the distribution in N_* for the OB groups (panel a) and O-star groups (panel b). Two slopes are shown fitted to the power-law distribution, weighted by the square root of the bin value, $\sqrt{N(\log N_*)}$: the solid line shows the fit for the entire distribution, yielding -2.51 ± 0.29 and -2.33 ± 0.42 for the OB and O-star samples, respectively; and the dotted line shows the fit omitting the first bin, which corresponds to single stars, resulting in fits of -2.27 ± 0.38 and -2.11 ± 0.55 for the OB and O-star samples, respectively. The fits omitting the single stars agree with the power-law slope of -2 (equation 1), found for the N_* distribution in a variety of systems, as discussed in §1. We again emphasize, as mentioned above, that the fitted slope has a dependence on the clustering distance d_s : for large d_s , more stars are drawn into the associations, causing the resultant slope of the clustering law to be flatter relative to clustering defined by a small d_s . Since we seek a characteristic value for the slope of $N(N_*)$, it is important to ensure that d_s is in turn characteristic of the sample. For the d_s in the extreme range of 20 – 40 pc (see Figure 2b), the O-star sample shows a variation in fitted slope, omitting the field stars, of -2.79 ± 0.84 to -1.85 ± 0.52 , respectively.

It is apparent that the single stars are slightly greater in number than the power law for the remainder of the N_* distribution, particularly in the OB sample. How significant is this excess in the isolated, “field” stars? We note that the magnitude of the excess may be a lower limit, since the slope of the N_* distribution is expected to flatten slightly at the smallest values of N_* , owing to statistical effects, as follows. We assume, as suggested above, that the OB stars counted in the value of N_* represent only the most massive stars for a population of star clusters that are in reality populated by a mass distribution described by a conventional IMF. Since we identified only OB stars, our clusters are selected with the criterion that each cluster contains a star of at least mass m_{cut} . The smallest, “unsaturated” clusters have a lower probability of having their maximum stellar mass $m_{\text{max}} \geq m_{\text{cut}}$, so they will be

TABLE 1
COMPARISON OF O-STAR CRITERIA

Cat ID ^a	Sp Type ^b	Identified ^c (y or n)	Cat ID ^a	Sp Type ^b	Identified ^c (y or n)
16828	O5 III(f)	y	53382	B0 IWW	y
38024	O5 V	y	54456	B0 IW	y
5869	O7 V	y	54958	B0 IIIWW	y
16056	O7 III	y	9079	B1.5 V	n
16885	O7 III	y	9488	B1 I	n
17457	O7 III	y	18700	B1 Ib	y
17927	O7.5Iaf+	y	37732	B1 IWW	n
19650	O7.5 III	y	42740	B1 III	n
22837	O7.5 V	y	43807	B1 V	n
40341	O7 III	y	44784	B1 III	n
43724	O7 V	y	45114	B1 III	y
45521	O7 If	y	45438	B1 Ve	n
46035	O7 III	y	45809	B1 III	n
52170	O7 V	y	50609	B1 III	n
27731	O8.5 V	y	51009	B1.5 III	n
43197	O8.5 V	y	53225	B1 V	n
43734	O8 V	n	26901	B2 IIIW	y
49580	O8.5 V	y	32907	B2 II	n
50825	O8 Vn	y	50826	B2.5 III	n
53373	O8.5 V	y	54818	B2 I	n
6406	O9+NEB	n	24929	B3 I	n
11777	O9 II	y	43844	B3 I	n
40610	O9 V	y	44828	B3 I	n
45677	O9 III	y	47028	B3 I	n
47540	O9 III	y	49606	B3 I	n
3459	B0 IWW	n	45722	B8 Ve	y
13075	B0.5 III	y	50475	B8 Iab	n
13831	B0.5 V	y	53084	B8-A0 I	n
15503	B0.5 V	n	5391	B pec	y
15742	B0 IWW	y	21801	B pec	y
18614	B0 IWW	n	24914	B extr	y
20656	B0 I	y	40851	B extr	y
23702	B0 IW	y	10915	A0 Ia	n
41648	B0.5 III	n	43215	A0 I	n
43686	B0.5 V	n	48732	A0 I	n
43758	B0.2 V	n	52992	A1 I	n
51575	B0 III	y

^aCatalog number from Massey (2002)

^bSpectroscopic type compiled by Massey (2002)

^cIdentified by O-star criteria equations 2 – 5

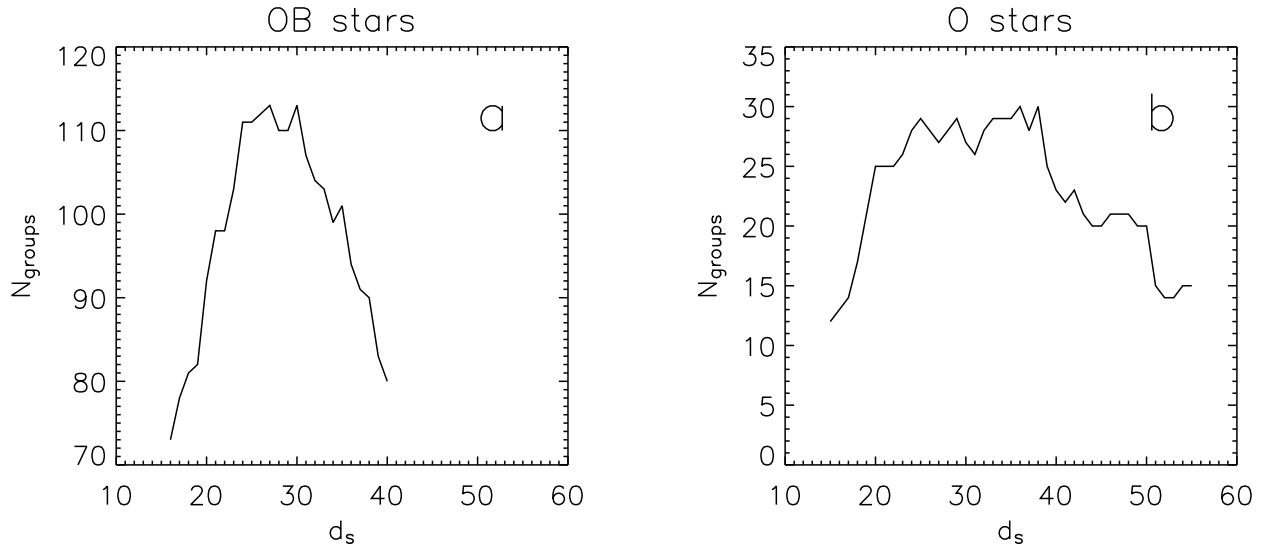


FIG. 2.— Number of groups with $N_* \geq 3$ as a function of clustering distance d_s for the OB sample (panel *a*) and O-star sample (panel *b*).

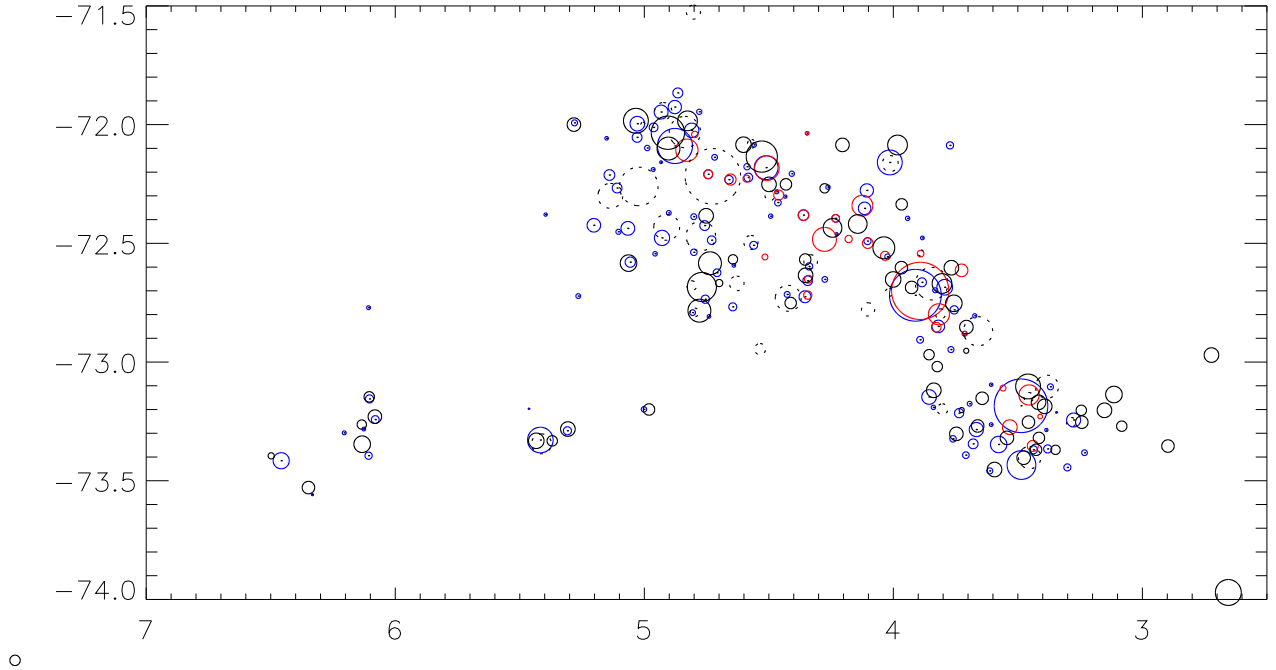


FIG. 3.— Centroids and sizes of associations identified by Hodge (1985; solid black), Battinelli (1991; dotted black), our OB sample (blue) and our O-star sample (red). Note that all blue circles have a dot at the center, thus overplotted identical circles can be identified by small dots in the center of red circles. (RA and Dec given in degrees of arc.)

TABLE 2
GROUPS FROM THE CANDIDATE OB SAMPLE

OB grp	RA	Dec	$D(\text{min})$	$D(\text{pc})$	N_*
20	11.3029	-73.3820	1.38	23.93	4
24	11.3639	-73.2441	3.39	58.90	5
29	11.5932	-73.1044	1.45	25.21	4
30	11.5857	-73.4439	1.69	29.37	3
31	11.5817	-73.2120	0.38	6.64	3
38	12.0545	-73.1842	12.91	224.68	70
40	11.7724	-73.2863	0.81	14.05	3
41	11.8078	-73.3658	1.97	34.36	4
45	12.0111	-73.3695	1.92	33.33	4
47	12.2249	-73.4337	6.93	120.56	26
64	12.2657	-72.0873	1.75	30.42	4
73	12.4821	-73.3470	3.95	68.70	16
74	12.4058	-73.0955	0.85	14.84	3
75	12.4251	-72.8051	1.02	17.81	3
86	12.5262	-73.2635	0.90	15.73	3
91	12.6156	-72.8806	1.16	20.18	4
98	12.6898	-73.4584	1.47	25.53	6
99	12.7466	-72.6852	3.78	65.71	9
100	12.6862	-72.7800	1.99	34.61	5
101	12.7490	-73.2845	3.42	59.56	10
104	12.7620	-73.1756	1.14	19.90	4
107	13.1672	-72.7186	12.48	217.09	55
110	12.8384	-73.3445	2.35	40.93	7
112	12.8514	-72.9475	1.46	25.40	3
115	12.8844	-72.6976	1.20	20.94	3
118	12.9530	-72.8498	3.02	52.62	7
119	12.8984	-72.4770	0.91	15.80	3
120	12.9375	-73.2152	2.21	38.45	8
121	12.9762	-73.3923	1.59	27.72	3
123	13.1031	-72.1594	5.99	104.24	15
125	13.0386	-72.6643	2.14	37.23	6
131	13.0357	-72.3948	1.05	18.26	3
137	13.1042	-73.3233	1.57	27.33	4
142	13.3029	-73.1472	3.52	61.32	8
150	13.2429	-72.9064	1.64	28.61	3
152	13.2756	-73.1909	1.06	18.42	3
158	13.4218	-72.5561	1.30	22.63	3
160	13.4898	-72.2771	3.20	55.66	6
170	13.5753	-72.3525	3.01	52.33	9
174	13.6399	-72.4905	1.70	29.66	4
195	13.9908	-72.3949	1.86	32.43	4
197	13.9913	-72.2634	1.06	18.43	3
204	14.0291	-72.4610	0.71	12.40	3
211	14.0923	-72.0363	0.82	14.26	3
228	14.3369	-72.6518	1.37	23.86	5
233	14.4076	-72.3812	2.52	43.93	5
235	14.4236	-72.2069	1.26	22.01	3
237	14.5052	-72.5974	1.74	30.22	5
241	14.5732	-72.6575	2.34	40.66	8
244	14.7403	-72.1810	5.74	99.90	42
247	14.6652	-72.7249	2.85	49.57	5
248	14.5854	-72.3032	0.78	13.66	3
255	14.6828	-72.2829	0.98	17.03	3
256	14.7037	-72.3284	1.59	27.67	3
263	14.8208	-72.0852	1.10	19.18	3
265	14.8466	-72.3857	1.06	18.47	3
270	14.8983	-72.7153	1.40	24.44	3
277	15.0082	-72.2228	2.09	36.34	4
279	14.9884	-72.1773	1.54	26.76	3
294	15.1744	-72.5081	1.87	32.59	4

TABLE 2
(*continued*)

OB grp	RA	Dec	$D(\text{min})$	$D(\text{pc})$	N_*
303	15.2701	-72.2317	2.02	35.18	4
315	15.3803	-72.1378	1.38	23.95	3
325	15.4218	-71.9461	1.28	22.21	3
327	15.5244	-72.2091	2.15	37.40	5
331	15.5112	-72.5928	0.88	15.30	3
333	15.5852	-72.0239	3.47	60.41	7
337	15.8589	-72.0899	8.45	147.10	79
340	15.6331	-71.8665	2.41	41.86	5
344	15.7216	-71.9261	3.20	55.77	4
345	15.6789	-72.7675	1.92	33.33	4
347	15.7562	-72.4252	2.35	40.82	6
348	15.7160	-72.4867	2.07	35.98	4
351	15.7653	-72.6240	1.86	32.41	3
354	15.9167	-71.9469	3.32	57.77	8
357	15.8683	-72.3877	1.43	24.85	3
365	16.0226	-72.7355	2.00	34.80	8
366	15.9992	-72.5378	1.54	26.85	4
367	16.0374	-72.8077	0.89	15.50	3
369	16.0700	-72.0117	2.11	36.70	4
373	16.1001	-72.1584	0.70	12.26	3
376	16.1858	-72.3718	1.15	20.02	3
377	16.2677	-71.9959	3.51	60.99	19
382	16.2279	-72.0984	1.30	22.70	4
383	16.2297	-72.1892	0.95	16.61	3
385	16.2451	-72.7920	1.36	23.67	5
388	16.3209	-72.0536	2.35	40.90	4
391	16.3701	-72.4773	3.66	63.75	8
399	16.5235	-72.5441	1.08	18.87	4
415	16.7752	-72.2671	2.34	40.67	5
416	16.7213	-72.0574	0.89	15.42	3
420	16.8253	-72.2122	2.59	45.08	5
421	16.7891	-72.4370	3.31	57.54	6
426	16.8895	-72.5793	2.48	43.11	5
429	16.9275	-72.4516	1.23	21.39	4
439	17.0803	-71.9925	1.43	24.93	3
444	17.2285	-72.4238	3.28	56.99	10
449	17.3037	-73.1992	1.29	22.40	4
460	17.7278	-72.7223	1.18	20.45	3
464	17.8254	-72.3788	0.79	13.72	4
480	18.4627	-73.2896	1.96	34.18	8
486	18.8834	-73.3285	6.18	107.50	24
496	18.9001	-73.1967	0.32	5.62	3
529	20.6192	-72.7708	0.96	16.66	3
538	21.0626	-73.1555	1.95	33.88	8
539	21.0881	-73.2422	1.88	32.75	4
546	21.2965	-73.2821	0.90	15.68	3
547	21.3705	-73.3945	1.73	30.09	4
550	21.5905	-73.2984	0.96	16.65	3
568	22.3738	-73.5585	0.52	8.98	3
569	22.6252	-73.4156	3.88	67.59	11
576	22.6252	-73.4156	3.88	67.59	11

TABLE 3
GROUPS FROM THE CANDIDATE O-STAR SAMPLE

O grp	RA	Dec	$D(\text{min})$	$D(\text{pc})$	N_*
8	11.9117	-73.1385	4.87	84.71	11
11	11.8196	-73.2295	1.11	19.35	3
13	12.0083	-73.3533	2.64	45.86	4
19	12.2742	-73.2744	3.57	62.11	6
24	12.2523	-73.1099	1.41	24.49	3
26	12.4694	-72.6139	3.03	52.78	4
38	12.6156	-72.8806	1.16	20.18	4
41	13.0895	-72.7004	13.76	239.45	57
45	12.9077	-72.7988	5.06	88.03	12
50	12.9830	-72.8530	2.30	40.07	4
51	12.9693	-72.5435	1.60	27.84	4
62	13.4522	-72.5525	2.19	38.11	4
67	13.5963	-72.3412	5.02	87.31	12
68	13.6438	-72.4994	2.52	43.85	5
76	13.8855	-72.4820	1.74	30.28	3
78	13.9908	-72.3949	1.86	32.43	4
81	14.2089	-72.4833	5.75	100.05	11
84	14.0923	-72.0363	0.82	14.26	3
97	14.4076	-72.3812	2.52	43.93	5
102	14.5581	-72.6512	1.87	32.61	4
104	14.7329	-72.1834	5.90	102.61	26
107	14.6211	-72.7179	2.00	34.71	3
109	14.6682	-72.2968	2.38	41.43	5
121	15.0359	-72.2274	1.72	29.92	3
124	15.0641	-72.5572	1.42	24.74	3
130	15.2501	-72.2311	2.68	46.59	5
143	15.5244	-72.2091	2.15	37.40	5
145	15.5583	-72.0413	1.55	26.96	3
146	15.7173	-72.1075	5.36	93.19	17

TABLE 4
GROUP MEMBERSHIP FOR THE CANDIDATE OB SAMPLE^a

RA	Dec	U	$U \text{ err}$	B	$B \text{ err}$	V	$V \text{ err}$	R	$R \text{ err}$	ID	OB grp
10.1171	-73.5425	14.01	0.05	14.96	0.04	15.00	0.03	14.96	0.07	107	1
10.1832	-73.4063	14.40	0.05	15.18	0.04	15.12	0.03	14.86	0.07	298	2
10.3880	-73.4256	14.24	0.06	15.15	0.06	15.28	0.04	15.30	0.11	1037	3
10.5417	-73.2323	13.44	0.03	14.42	0.03	14.60	0.02	14.69	0.05	1600	4
10.5515	-73.3866	14.26	0.05	15.19	0.04	15.15	0.03	15.04	0.08	1631	5

^aThe complete version of this table is in the electronic edition of the Journal. The printed edition contains only a sample.

TABLE 5
GROUP MEMBERSHIP FOR THE CANDIDATE O-STAR SAMPLE^a

RA	Dec	U	$U \text{ err}$	B	$B \text{ err}$	V	$V \text{ err}$	R	$R \text{ err}$	B5	B5 err	ID	O grp
11.1440	-73.1597	13.78	0.05	14.70	0.04	14.82	0.03	14.74	0.07	11.92	0.05	4424	1
11.2379	-73.0130	13.19	0.03	14.30	0.03	14.36	0.02	14.29	0.04	11.16	0.09	4922	2
11.2438	-73.0213	14.05	0.05	14.94	0.04	14.91	0.03	14.86	0.07	12.19	0.05	4949	2
11.3259	-73.2564	12.45	0.02	13.36	0.01	13.31	0.01	13.14	0.02	10.25	0.08	5391	3
11.3867	-73.0773	13.16	0.04	14.15	0.04	14.30	0.03	14.28	0.06	10.85	0.06	5718	4

^aThe complete version of this table is in the electronic edition of the Journal. The printed edition contains only a sample.

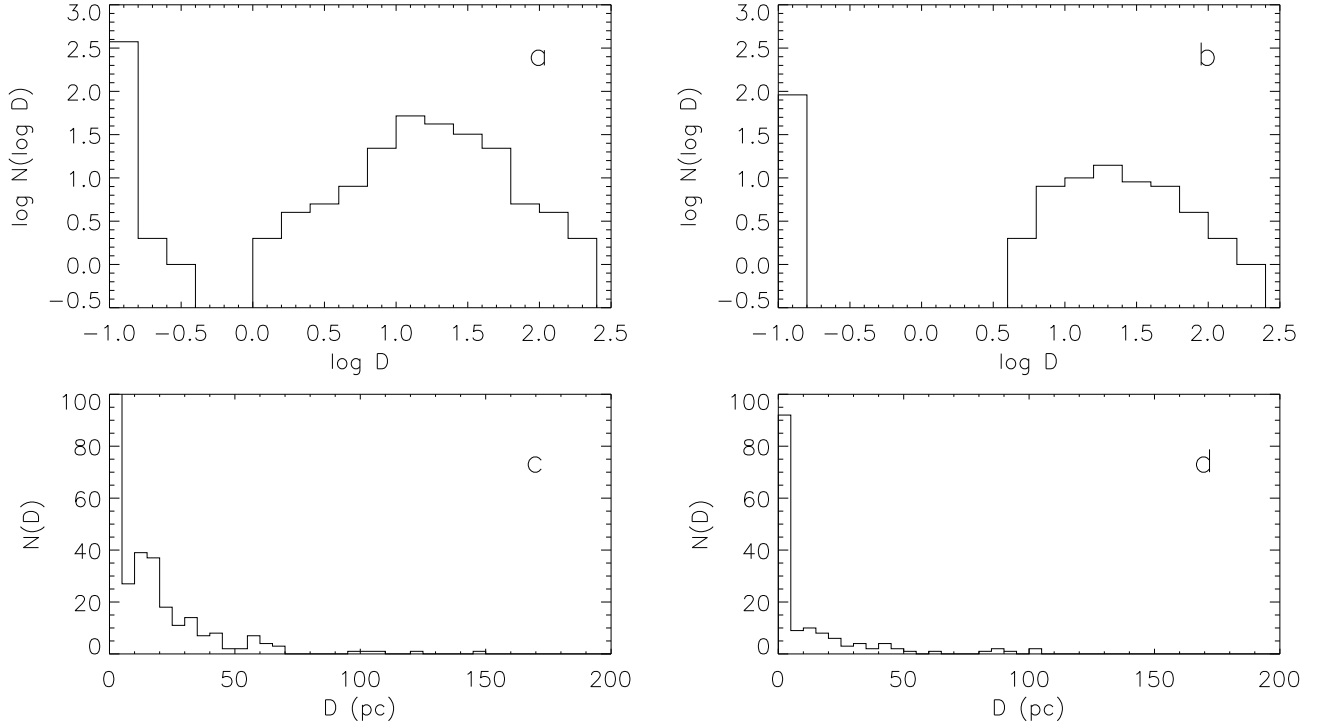


FIG. 4.— Logarithmic size distribution for groups identified from the candidate OB and O-star samples are shown in the top row (panels *a* and *b*, respectively). The linear distributions for the OB and O-star samples are shown in the bottom row (panels *c* and *d*, respectively). The first bin in Figure 4c has a maximum of 391.

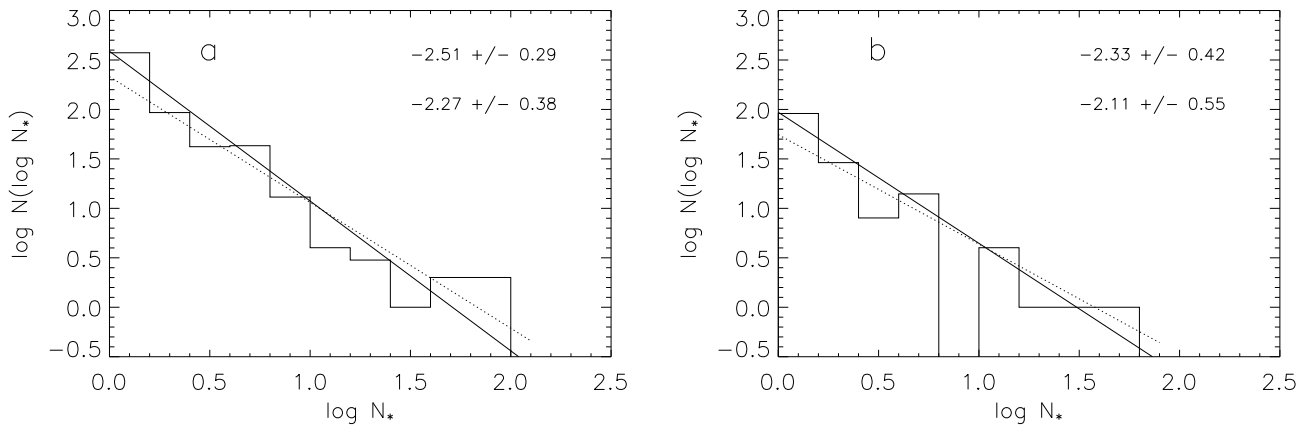


FIG. 5.— The distribution in N_* for groups defined from the candidate OB sample (panel *a*) and O-star sample (panel *b*). Fits to the power-law exponent ($-\beta$) are shown for the entire distributions (upper values) and omitting the first bin of single stars (lower values). Note that the slope fitted in logarithmic space is $-\beta + 1$.

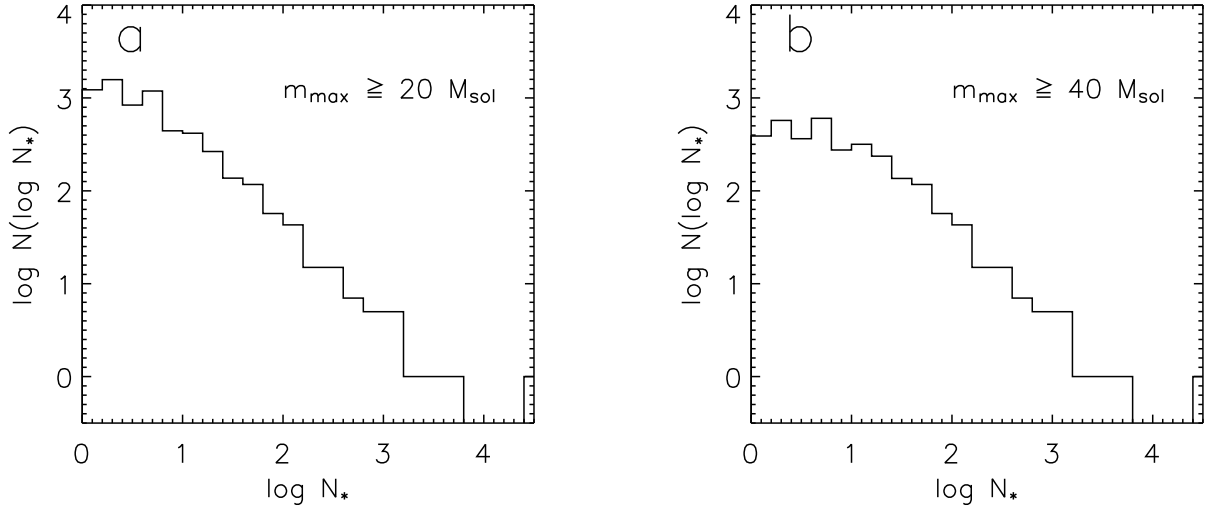


FIG. 6.— Monte Carlo models for distributions of $\log N_*$, selected by the criterion that the maximum stellar mass in each cluster be at least $m_{\max} \geq m_{\text{cut}}$, showing $m_{\text{cut}} = 20 M_{\odot}$ and $40 M_{\odot}$ in panels *a* and *b*, respectively.

progressively missing from a sample of clusters selected in this way (see Oey & Clarke 2003 for a detailed discussion of this effect).

Figure 6 shows Monte Carlo models that demonstrate this effect. N_* is drawn from a power-law distribution of slope -2 (equation 1), with the individual stellar masses drawn from a Salpeter (1955) IMF having $10 \leq m \leq 100 M_{\odot}$. Figure 6*a* shows the distribution in N_* for 10,000 clusters having at least one star with mass $m_{\max} \geq 20 M_{\odot}$, and Figure 6*b* is the same, but selected for $m_{\max} \geq 40 M_{\odot}$. We see a flattening in the distributions for small N_* , and the flattening is stronger in Figure 6*b*, since the probability of drawing a $40 M_{\odot}$ star is less than for a $20 M_{\odot}$ star.

Figure 7 shows the stellar density of all catalogued stars in the *UBVR* survey as a function of radius around the isolated, field massive stars found in the OB (solid line) and O-star (dashed line) samples. The errors are computed as $\sqrt{\bar{n}}/\pi r^2$ for the total n stars within radius r , omitting the central field massive stars. As seen in Figure 7, it is apparent that the stellar density increases at small r . This is consistent with our suggestion that most massive field stars represent the most massive component of groups of smaller stars, as is expected from the stellar IMF.

Another effect that can offset the statistical flattening in the form of the N_* distribution for small N_* , is evolution. In the most extreme situation, we consider that all the OB associations in the SMC were formed together in a single burst of global star formation. Staveley-Smith et al. (1997) find that the H I shells identified in the SMC appear to have a narrow age distribution around 5 Myr. We described above that the unsaturated, lowest- N_* clusters have a lower average stellar mass (e.g., Oey & Clarke 2003). Since stellar lifetimes are longer for lower-mass stars, we therefore expect that these unsaturated clusters will tend to last longer, on average, than the statistically fully-sampled, or saturated, objects. Thus, we may expect that the distribution in N_* steepens with time.

We constructed Monte Carlo simulations of such an aging burst of clusters. Figure 8 shows the models for a

population of clusters at 0, 15, and 25 Myr after their simultaneous formation. We used the same IMF parameters as before, and the stellar ages are from the grid of Charbonnel et al. (1993) for SMC metallicity. Each of the model N_* distributions is fitted with a power-law slope, shown in Figure 8. We see that, while it is difficult to discern the slope steepening over the entire sample after 15 Myr, and even at 25 Myr, it is apparent that the aging effect is most pronounced in the smallest N_* bins, and that the $N_*=1$ bin becomes the most disproportionately enhanced. For continuous creation of the clusters, the net observed slope will be intermediate between the forms in Figure 6 and Figure 8.

The modest observed excess of single stars is also likely to be caused in part by a contribution to their population by runaway OB stars. If runaway OB stars originate in associations, however, then this contribution must be small, since runaways correspond to about 3% and 20% of field early B and early O stars, respectively (Blaauw 1961). Runaways will contribute primarily to the single-star population, while binary runaways represent $\lesssim 19\%$ of all runaways (Gies 1987). Binary runaways are likely to be tight pairs that remain unresolved in the 0.67 pc px^{-1} survey resolution.

It is also possible that spurious selection of candidate stars, owing to the coarse photometric criteria, are a factor. We showed in §2 that there may be a net of about 15% of the O-star sample that consist of spuriously selected B stars; while in principle, these should be distributed proportionately between clusters and the field, it is possible that crowding effects in clusters favor field selection. If so, owing to the longer lifetimes of B stars, they could contribute disproportionately to the field star population. However, we emphasize that this requires a significant variation in the spatial distribution of only the spurious candidates, between field and clusters.

The most important factor in enhancing the field star population, however, is probably the strong variation in star formation density across the SMC. The highest star

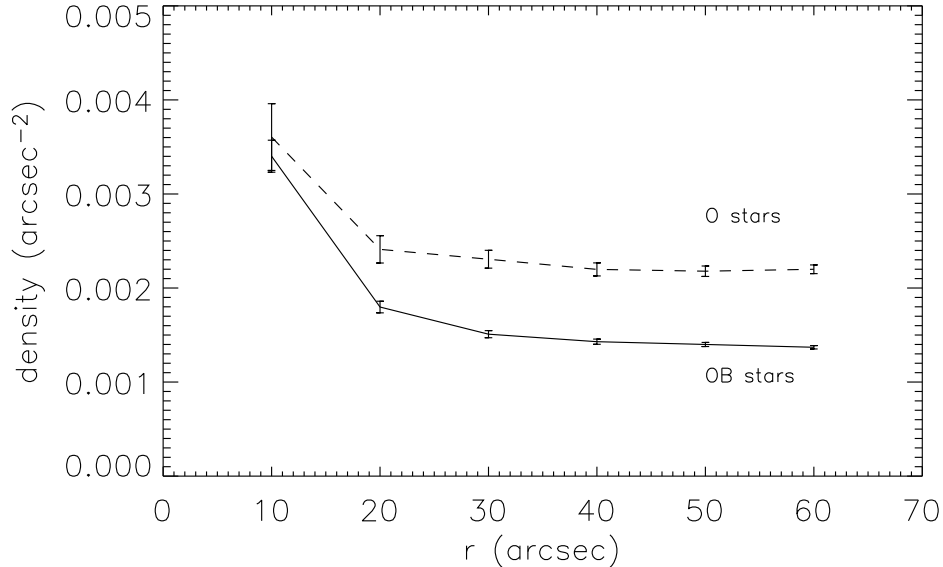


FIG. 7.— Mean stellar density (arcsec $^{-2}$) within radius r (arcsec) from isolated massive stars in the candidate OB (solid line) and O-star (dashed line) samples ($10'' = 2.9$ pc). The O-star sample shows a higher background density since that sample is limited to the SMC bar region (Figure 1).

formation density occurs in the SMC bar, where, as seen in Figure 3, most of the associations are located. Individual massive field stars, on the other hand, have a much more uniform distribution, as seen in Figure 9. The uneven star formation density distribution in this galaxy therefore favors the field stars and enhances the $N_* = 1$ bin for the OB sample in Figure 5. The effect is much less pronounced in the O-star sample, which is limited to the SMC bar region.

Considering these effects, it is apparent that there is no strong variation or change in character of the power-law distribution seen in Figure 5 for the smallest values of N_* . The empirical samples (Figure 5) are much smaller than those in the models and therefore have significantly poorer statistics in $\log N(\log N_*)$. Thus, the modeled effects will be more difficult to discern in the data. Since our results are largely consistent with a single intrinsic power-law form for the clustering law, this suggests that the massive field star population simply represents an extension of the massive cluster population extending down to $N_* = 1$. There is no evidence that the majority of massive field stars originate from a mode of star formation that is different from those in associations. However, further studies of massive field and cluster populations in other environments are necessary to confirm the generality of these results.

5. DISCUSSION

For a universal IMF, the constant slope of the N_* distribution extending to the field stars has profound consequences for their global feedback influence in galaxies. We can now quantify the assertion that most massive stars form in associations: for an N_* distribution given by equa-

tion 1, the total number of OB stars is,

$$N_{*,\text{tot}} \propto \sum_{N_*=1}^{N_{*,\text{up}}} N_* \cdot N_*^{-2} \quad , \quad (9)$$

where $N_{*,\text{up}}$ refers to the upper-limit, maximum cluster of stars. Equation 9 corresponds to a divergent harmonic series which can be approximated for large $N_{*,\text{up}}$ as:

$$N_{*,\text{tot}} \approx \ln N_{*,\text{up}} + \gamma \quad , \quad (10)$$

where $\gamma \simeq 0.5772$ is the Euler-Mascheroni constant. Thus the fraction of $N_* = 1$ field stars is $(\ln N_{*,\text{up}} + \gamma)^{-1}$ of the total $N_{*,\text{tot}}$. For our OB and O star samples, respectively, $\log N_{*,\text{up}} \simeq 2.0$ and 1.8, yielding 19% and 21% fractions for the field stars.

Counting the actual stars in our OB and O star samples, we find that 374 and 91 candidates, respectively, had no massive companions within the clustering radius. These correspond to 28% and 24%, reflecting the excess found above. These fractions are about a factor two lower than the finding by Parker et al. (2001) that over half of their *UIT*-selected candidate O stars are outside catalogued association boundaries in the Large Magellanic Cloud (LMC). The results for both the SMC and LMC may be odds with the results of Massey et al. (2002), who found a much steeper IMF slope for field vs cluster massive stars: a steeper IMF slope in the field would be manifested as a smaller number of field OB stars, yet the slope of the N_* distribution tends to be steeper than expected, rather than flatter. If the field star IMF is indeed steeper than in clusters, then the clustering law must also steepen substantially for the smallest clusters, in such a way as to compensate for a steep IMF in our data. Further investigation is necessary to resolve this issue.

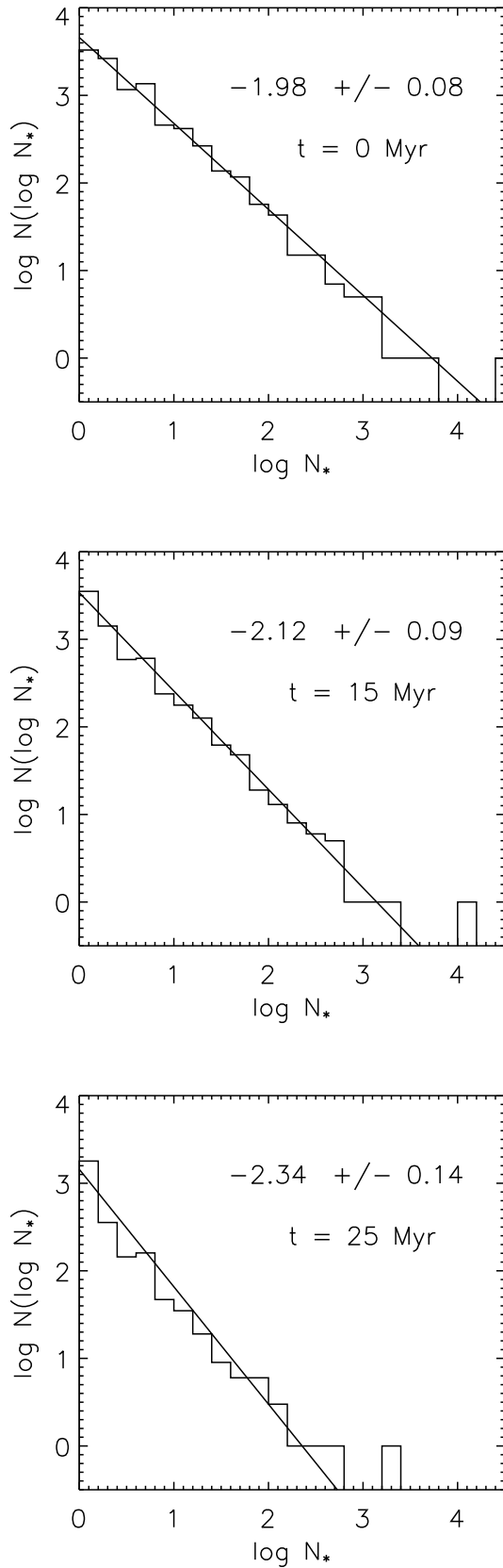


FIG. 8.— Monte Carlo models for evolution in the $\log N_*$ distribution, assuming that all objects were created simultaneously. Models for ages of 0, 15, and 25 Myr are shown, with fitted power-law slopes. As in Figure 5, the linear power-law exponents are shown, while the fitted slope is $-\beta + 1$ in logarithmic space.

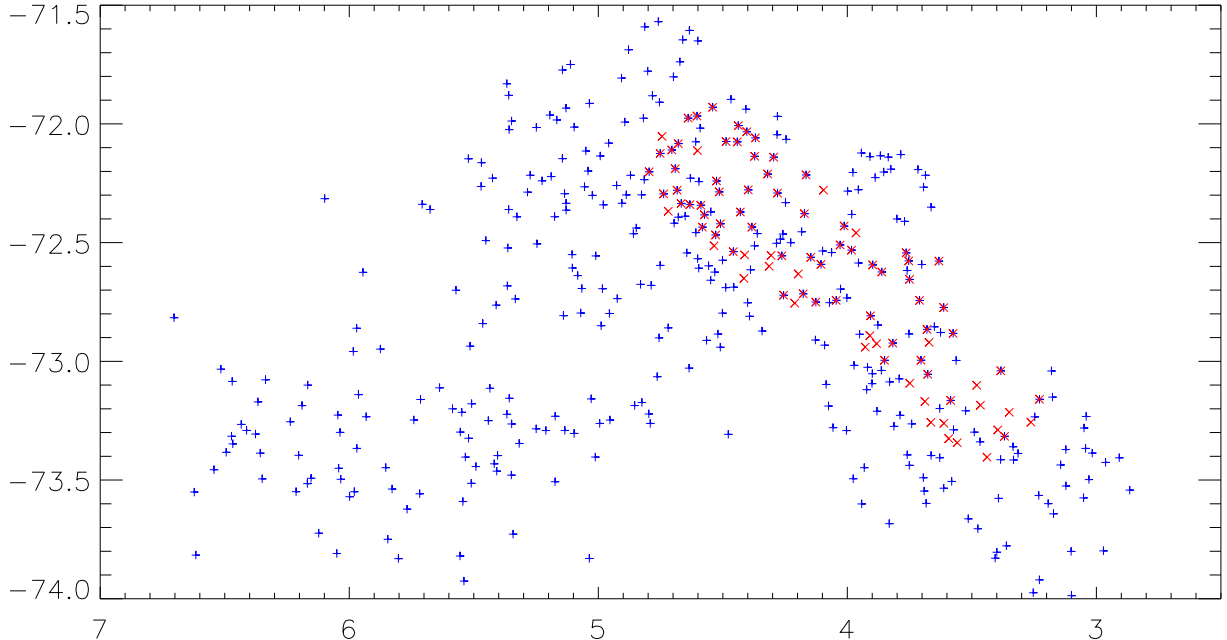


FIG. 9.— Spatial distribution of isolated field stars for the OB sample (plus symbols), and O-star sample (cross symbols). Scale and axes are as in Figure 3.

In the meantime, the data appear to be broadly consistent with the simpler scenario of, *simultaneously*, a universal IMF and universal clustering law given by equation 1. As emphasized by McKee & Williams (1997), the total OB star population, and thus the fraction of isolated field massive stars, is driven by $N_{*,\text{up}}$ with an inverse logarithmic dependence. For maximum $N_{*,\text{up}}$ ranging between 10 and 10^6 , equation 10 yields a fraction of field OB stars ranging from 35% to 7%, respectively.

The clustering law in equation 1 has important consequences for feedback, implying that the interstellar porosity caused by the formation of superbubbles and supernova remnants has equal relative contributions from objects of all sizes (Oey & Clarke 1997). And, since the Strömgren volume $V_s \propto N_*$, it also implies that a strong majority of the field massive stars likely contribute to ionizing the diffuse, warm ionized medium, which constitutes about 40% of the total $H\alpha$ luminosity in star-forming galaxies (e.g., Waltherbos 1998). Our result is quantitatively consistent with the result of Hoopes & Waltherbos (2000) that field OB stars can power $40\% \pm 12\%$ of the warm ionized medium in M33, where the fraction of field OB stars is likely around 15%.

6. CONCLUSION

We find no evidence that the field massive stars in the SMC are formed by a fundamentally different star-forming

process. Rather, we find that the continuous power-law distribution in N_* down to $N_*=1$ strongly suggests that the star-forming process is continuous from rich clusters to poor groups, apparently for all ensembles that form OB stars. The data are consistent with the model that single, field OB stars are usually the most massive member of a group of smaller stars, as expected from the universal N_* distribution (equation 1). These results are consistent with the *simultaneous* existence of a universal IMF and universal N_*^{-2} clustering law. These joint universal power laws imply that field OB stars constitute roughly 35% to 7% of the total massive star population, with an inverse logarithmic dependence on $N_{*,\text{up}}$ of the most populous cluster. Thus, the fraction is dependent on galaxy size and/or star formation rate. The contribution of these field stars to the ionized volume in the warm ionized medium is likely to scale according to their relative fraction. The universal clustering law also implies equal relative contributions by superbubbles of all sizes to the interstellar porosity.

We are pleased to acknowledge discussions with René Waltherbos, Cristiano Porciani, Todd Small, and especially, Chris McKee and the anonymous referee. We also thank Phil Massey for generously providing the $UBVR$ data in advance of publication. This work was supported by the NASA Astrophysics Data Program, grant NAG5-10768.

REFERENCES

- Azzopardi, M. & Vigneanu, J. 1982, *A&AS*, 291
 Battinelli, P. 1991, *A&A*, 244, 69
 Blaauw, A. 1961, *Bull. Astron. Inst. Netherlands*, 15, 265
 Bothun, G. D. & Thompson, I. B. 1988, *AJ*, 96, 87
 Charbonnel, C., Meynet, G., Maeder, A., Schaller, G., & Schaerer, D. 1993, *A&A*, 101, 415
 Cardelli, J. A., Clayton, G. C., & Mathis, J. S. 1989, *ApJ*, 345, 245
 Dolphin, A. E., Walker, A. R., Hodge, P. W., Mateo, M., Olszewski, E. W., Schommer, R. A., & Suntzeff, N. B. 2001, *ApJ*, 562, 303

- Elmegreen, B. G. & Efremov, Y. N. 1997, ApJ, 480, 235
Feast, M. W., Thackeray, A. D., & Wesselink, A. J. 1960, MNRAS, 121, 337
Gies, D. R. 1987, ApJS, 64, 545
Harris, W. E. & Pudritz, R. E. 1994, ApJ, 429, 177
Hodge, P. W. 1985, PASP, 97, 530
Hoopes, C. G. & Waltherbos, R. A. M. 2000, ApJ, 541, 597
Hunter, D. A., Elmegreen, B. G., Dupuy, T. J., & Mortonson, M. 2003, AJ, 126, 1836
Kennicutt R. C., Edgar B. K., & Hodge P. W., 1989, ApJ, 337, 761
Kroupa, P. & Weidner C. 2003, ApJ, in press; astro-ph/0308356
Landolt, A. U., 1992, AJ, 104, 340
Li, Y., Klessen, R. S., & Mac Low, M.-M. 2003, ApJ, 592, 975
Lucke, P. B. & Hodge, P. W. 1970, AJ, 75, 171
Massey, P., 2002, ApJS, 141, 81
McKee, C. F. & Williams, J. P. 1997, ApJ, 476, 144
Meurer, G. R., Heckman, T. M., Leitherer, C., Kinney, A., Robert, C., & Garnett, D. R. 1995, AJ, 110, 2665
Oey, M. S. & Clarke, C. J. 1997, MNRAS, 289, 570
Oey, M. S. & Clarke, C. J. 1998, AJ, 115, 1543
Oey, M. S. & Clarke, C. J. 2003, in preparation
Oey, M. S. & Muñoz-Tuñón, C. 2003, in *Star Formation Through Time*, eds. E. Pérez, R. González Delgado, & G. Tenorio-Tagle, (San Francisco: ASP), 61
Parker, J. W., Cornett, R. H., & Stecher, T. P. 2004, in preparation
Parker, J. W., Hill, J. K., Cornett, R. H., et al. 1998, AJ, 116, 180
Parker, J. W., Zaritsky, D., Stecher, T. P., Harris, J., & Massey, P. 2001, ApJ, 121, 891
Salpeter E. E. 1955, ApJ, 121, 161
Sanduleak, N. 1969, Contr. Cerro-Tololo Interamerican Obs., 89
Staveley-Smith, L., Sault, R. J., Hatzidimitriou, D., Kesteven, M. J., & McConnell, D. 1997, MNRAS, 289, 225
Zhang, Q. & Fall, S. M. 1999, ApJ, 527, L81